

Effect of metal plate on ultrasonic cavitation field distribution

Jin-He Liu(刘金河), Zhuang-Zhi Shen(沈壮志), Peng-Fei Cao(曹鹏飞), Jian-Feng Li(李建锋), and Xiao-Qiang Bai(白小强)

Citation: Chin. Phys. B, 2025, 34 (**5**): 054302. DOI: 10.1088/1674-1056/adca9d
http://cpb.iphy.ac.cn; http://iopscience.iop.org/cpb

What follows is a list of articles you may be interested in

Behaviors of cavitation bubbles driven by high-intensity ultrasound

Chen-Yang Huang(黄晨阳), Fan Li(李凡), Shi-Yi Feng(冯释毅), Cheng-Hui Wang(王成会), Shi Chen(陈时), Jing Hu(胡静), Xin-Rui He(何芯蕊), and Jia-Kai Song(宋家凯)
Chin. Phys. B, 2024, 33 (**2**): 024301. DOI: 10.1088/1674-1056/ad0717

Bubble nucleation in spherical liquid cavity wrapped by elastic medium

Xian-Mei Zhang(张先梅), Fan Li(李凡), Cheng-Hui Wang(王成会), Jing Hu(胡静), Run-Yang Mo(莫润阳), Zhuang-Zhi Shen(沈壮志), Jian-Zhong Guo(郭建中), and Shu-Yu Lin(林书玉)
Chin. Phys. B, 2023, 32 (**6**): 064303. DOI: 10.1088/1674-1056/acaa30

Effects of adjacent bubble on spatiotemporal evolutions of mechanical stresses surrounding bubbles oscillating in tissues

Qing-Qin Zou(邹青钦), Shuang Lei(雷双), Zhang-Yong Li(李章勇), and Dui Qin(秦对)
Chin. Phys. B, 2023, 32 (**1**): 014302. DOI: 10.1088/1674-1056/ac70ba

Effect of nonlinear translations on the pulsation of cavitation bubbles

Lingling Zhang(张玲玲), Weizhong Chen(陈伟中), Yang Shen(沈阳), Yaorong Wu(武耀蓉), Guoying Zhao(赵帼英), and Shaoyang Kou(寇少杨)
Chin. Phys. B, 2022, 31 (**4**): 044303. DOI: 10.1088/1674-1056/ac1e18

Tunable acoustic radiation pattern assisted by effective impedance boundary

Feng Qian(钱 枫), Li Quan(全力), Li-Wei Wang(王力维), Xiao-Zhou Liu (刘晓宙), Xiu-Fen Gong(龚秀芬)
Chin. Phys. B, 2016, 25 (**2**): 024301. DOI: 10.1088/1674-1056/25/2/024301

Effect of metal plate on ultrasonic cavitation field distribution

Jin-He Liu(刘金河)[1,†], Zhuang-Zhi Shen(沈壮志)[2], Peng-Fei Cao(曹鹏飞)[1], Jian-Feng Li(李建锋)[1], and Xiao-Qiang Bai(白小强)[1]

[1] *School of New Energy, Longdong University, Qingyang* 745000, *China*
[2] *School of Physics and Information Technology, Shaanxi Normal University, Xi'an* 710119, *China*

(Received 20 January 2025; revised manuscript received 16 March 2025; accepted manuscript online 9 April 2025)

In order to enhance the ultrasonic degradation rate of organic solutions, a metal plate is placed at the water–air interface of the ultrasonic cleaning tank. Initially, the distribution of the acoustic field in the ultrasonic water tank was calculated using the simulation software COMSOL. The simulation results demonstrated that the utilization of the metal plate can eliminate the standing-wave acoustic field to a certain extent. Subsequently, the pixel method was selected for a quantitative comparison of the cavitation area in the flume with and without the metal plate. The results demonstrated that, under specific conditions, the area of ultrasonic cavitation in the water tank can be expanded using a metal plate. Thereafter, an acoustic degradation experiment was designed to confirm the feasibility of the simulation method. Furthermore, the impacts of the amplitude of the incident ultrasonic pressure, frequency, and the height of the liquid level in the water tank on the cavitation area were investigated.

Keywords: ultrasonic degradation rate, metal plate, cavitation, height of the liquid level

PACS: 43.20.+g, 43.35.+d, 43.38.+n

DOI: 10.1088/1674-1056/adca9d **CSTR:** 32038.14.CPB.adca9d

1. Introduction

With the rapid development of industrialization and the acceleration of urbanization, the problem of water pollution has become increasingly severe in China. According to statistics, the amount of industrial wastewater generated in China exceeds several hundred billion tons per year, and industrial wastewater is a major source of sewage.[1] In large-scale industrial production, wastewater comes from industrial sources, such as chemical, papermaking, textile, and metallurgical industries. These wastewaters contain a large amount of toxic organic pollutants, which pose a significant threat to human life and health.[2] Therefore, seeking a simple, efficient, and green sewage treatment method is of great significance for human health and sustainable socioeconomic development.

A wide range of conventional sewage treatment methodologies has been developed, such as physical,[3,4] chemical,[5–7] and biological methods.[8,9] However, these conventional treatment methods have been criticized for their low treatment efficiency and complicated operational processes, which have been shown to result in the formation of new harmful substances, thus causing secondary environmental pollution. In light of these challenges, there has been a notable focus on advanced oxidation processes (AOPs) in recent years, which have emerged as a significant area of research interest due to their high degradation efficiency and the absence of by-product formation compared to conventional methods.[10,11] The working mechanism of AOPs is to use hydroxyl radicals to oxidize organic pollutants in water into H_2O, CO_2, and inorganic salts. AOPs are largely divided into photocatalytic processes,[12] chemical oxidation,[13] electrochemical oxidation,[14] ozonation,[15] the Fenton oxidation reaction,[16] and ultrasound methods,[17] depending on how the hydroxyl radicals are produced. Ultrasound has many outstanding advantages: safety, cleanliness, high efficiency, a wide application range, and the absence of secondary pollutants compared with other methods.[18]

The functioning of ultrasound technology is based on the generation of hydroxyl radicals by ultrasonic cavitation, which serves to oxidize and decompose organic pollutants in sewage. Ultrasonic cavitation refers to the process in which microbubbles in the liquid are continuously expanded and contracted by ultrasonic waves, ultimately collapsing and rupturing.[17] High temperatures and pressures are generated, and hydroxyl radicals are formed when the bubbles collapse. The main factors influencing the ultrasonic degradation rate include acoustic intensity, ultrasound frequency and waveform type, solution temperature, and pH value. Therefore, a large amount of research has focused on analyzing the influence of the acoustic field characteristics in the cleaning tank on the degradation rate of organic pollutants.[19]

To further enhance the ultrasonic degradation rate of organic solutions, Ren *et al.*[20] installed ultrasonic transducers on both sides of the cleaning tank and set the distance between the transducers on both sides to an integer multiple of a quarter wavelength to eliminate the cleaning blind area. Wei *et al.*[21] used the simulation software COMSOL to numerically simulate the acoustic field characteristics of a larger-scale sonore-

†Corresponding author. E-mail: qy1451785880@163.com

© 2025 Chinese Physical Society and IOP Publishing Ltd. All rights, including for text and data mining, AI training, and similar technologies, are reserved.

actor containing a multi-stepped ultrasonic horn and designed a hydrophone measurement experiment to verify the simulation results. Zhang *et al.*[22] explored the influence of the direction of the incident acoustic wave on the characteristics of the acoustic field. The calculation results demonstrated that setting an appropriate direction for the incident acoustic wave can significantly improve acoustic intensity. Rashwan *et al.*[23] numerically simulated the effects of acoustic wave frequency, transducer probe position, and acoustic power on acoustic pressure. Liu *et al.*[24] improved the distribution characteristics of the acoustic field by means of mechanical stirring. However, these methods are complex and highly energy consuming. Therefore, a metal plate with a specific shape is proposed in this paper to expand the acoustic cavitation area in the ultrasonic water tank, thus further improving the acoustic degradation rate of organic solutions. The method proposed in this paper has the advantages of being simple to operate and having low energy consumption.

This paper proposes a novel methodology for the design of a water tank cover structure, the purpose of which is to modify and eradicate the acoustic standing wave field in order to enhance the uniformity of the acoustic field distribution. Furthermore, based on the theory of cavitation volume proposed by Zhai *et al.*[25] the ratio of the cavitation area to the non-cavitation area is calculated using the pixel method.

2. Methods

2.1. Experimental details

2.1.1. Materials

Rhodamine B (Rh B, $C_{28}H_{31}ClN_2O_3$, CAS: 81-88-9, AR) was purchased from Shanghai Macklin Biochemical Technology Co., Ltd (Macklin, Shanghai, China) and used as the material to be degraded without further purification. Pure water was used in all procedures and experiments.

2.1.2. Apparatus and procedure

A 40 mg/L solution of Rhodamine B was sonicated using a 40 kHz ultrasonic cleaner (SBL-150DTN, Ningbo Xinyi Ultrasonic Equipment Co., Ltd, China) at a power of 60W. A constant low-temperature tank (YHD-0506, Ningbo Yiheng Limited Company, China) was connected to the ultrasonic cleaner to maintain the temperature inside the ultrasonic tank at 24 °C. The ultrasonic cleaner and the metal cover are illustrated in Fig. 1(a). The thickness of the metal plate was 1 mm. The absorbance of the Rhodamine B solution was recorded by an ultraviolet–visible (UV-vis) spectrophotometer (UV2365, Uniko (Shanghai) Instrument Co., Ltd, China) at 30-min intervals. The wavelength range was 190–1100 nm. The degradation rate (DR) was calculated using

$$\mathrm{DR}(\%) = \frac{A_0 - A_t}{A_0} \times 100, \tag{1}$$

where A_0 and A_t are the initial and final absorbances of Rhodamine B, respectively.

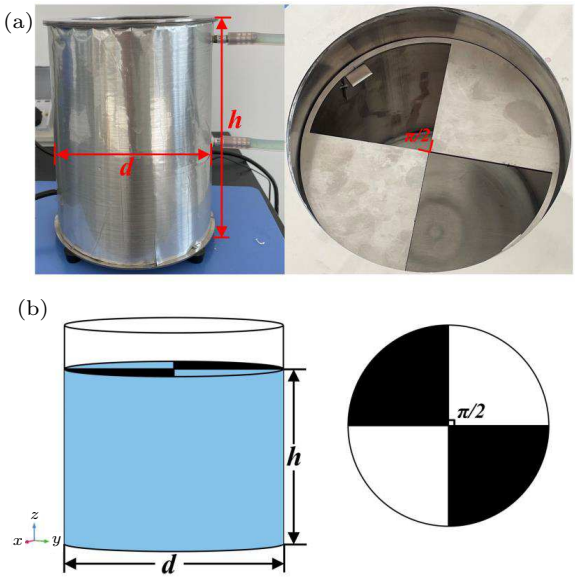


Fig. 1. Ultrasound cleaner: (a) photographs, (b) simulation diagrams.

2.2. Computational method

COMSOL Multiphysics is general-purpose simulation software that has frequently been employed to calculate the acoustic field distribution in a certain space. The Pressure Acoustics module of the simulation software is used to simulate the acoustic field distribution in an ultrasonic water sink.[26] The Pressure Acoustic module can perform simulations in the frequency domain or the time domain; the time domain is selected for more accurate calculation results. The entire simulation procedure is divided into three main phases: construction of computational models, setting of boundary conditions, and post-processing of results. The following is a detailed introduction to the three phases.

The ultrasound transducer has an operational working frequency of 40 kHz, and is mounted at the bottom of the sonoreactor. The calculation model with the metal plate placed at the water–air interface of the ultrasonic sink is shown in Fig. 1(b), where the metal plate is shown in black and air is shown in white; the metal plate is freely placed on the water–air interface. The metal plate used here is made from thin stainless steel, so the metal plate is simplified to a two-dimensional plate in the simulation process, without considering its thickness. The physical parameters used in the calculation are listed in Table 1, where C_a stands for the speed of ultrasonic waves in air, C_w the speed of ultrasonic waves in water, d the inside diameter of the sink, h the height of the sink, p_i the amplitude of the acoustic pressure, ρ_a the density of air, ρ_w the density of water and f the acoustic frequency.

At the physical interface, the Pressure Acoustics, Transient module is used to calculate the pressure change of acoustic waves propagating through the fluid under static background conditions. The governing equation of the physical

interface is given by

$$\frac{1}{\rho c}\frac{\partial^2 p}{\partial t^2}+\nabla\cdot(-\frac{1}{\rho}\nabla p)=0, \tag{2}$$

where p is the acoustic pressure, ρ is the density, and c is the speed of sound. The acoustic field within the water is numerically simulated according to the acoustic wave equation expressed in Eq. (2), which governs the propagation of acoustic waves through a material medium.[27] T is the acoustic period, and the value of T is 2.5×10^5 s based on $T=1/f$. The maximum cell in the mesh is 5 mm in size, and the minimum cell is 4 mm in size. The resolution of the narrow area is 0.85. The total time calculated is $20T$ and the time step is $T/50$. The finite-element software COMSOL Multiphysics 5.4 is employed to solve Eq. (2).

Table 1. Parameters used in the simulation calculation.

Parameter	Unit	Value
d	cm	12
h	cm	12
$P_{\rm i}$	Pa	1.5×10^5
$C_{\rm a}$	m/s	340
$C_{\rm w}$	m/s	1500
$\rho_{\rm a}$	kg/m^3	1.29
$\rho_{\rm w}$	kg/m^3	1000

2.2.1. Boundary conditions

To simplify the calculation, plane wave radiation boundary conditions are set on the bottom of the cylindrical sink to replace the ultrasonic wave emitted by the transducer. The expression for the plane wave is

$$p=p_{\rm i}\sin\left[2\pi f\left(t-\frac{\boldsymbol{r}\cdot\boldsymbol{e}_k}{c\,|\boldsymbol{e}_k|}\right)\right], \tag{3}$$

where $p_{\rm i}$ is the amplitude of the acoustic pressure, f is the acoustic frequency, c is the speed of the acoustic wave, and $\boldsymbol{e}_k$ is the wave direction vector.

The side walls of the tank are treated as acoustic hard boundaries. The metal plate consists of a metal area and an air area. The metal area is set as the acoustic hard boundary, and the air area is set as the acoustic soft boundary at the water–air interface of the ultrasonic sink. The water–air interface is approximately regarded as the acoustic soft boundary because the acoustic impedance of water is far greater than that of air. This is evident when the ultrasonic wave propagates from water to the water–air interface of the ultrasonic sink. The mathematical expression for the acoustic soft boundary is given below:

$$p=0. \tag{4}$$

The water–metal interface is approximately regarded as the acoustic hard boundary, since the acoustic impedance of water is far less than that of metal when the ultrasonic wave propagates from water to the water–metal interface of the ultrasonic sink. The mathematical expression for the acoustic hard boundary is

$$\frac{\partial p}{\partial \boldsymbol{n}}=0. \tag{5}$$

2.2.2. Post-processing

Acoustic cavitation occurs when the ultrasonic pressure amplitude exceeds the cavitation threshold, which is approximately 1 atm under atmospheric pressure at room temperature.[28] Therefore, based on the acoustic field distribution simulated, the cavitation area diagram for any section in the flume can be obtained at a certain moment using the logical expression. The distribution of the acoustic field in the tank exhibits a certain periodicity in time, and the maximum value of the acoustic pressure (acoustic pressure amplitude) occurs twice during an acoustic period, so the period of the cavitation region diagram in time is half of the acoustic period. For this reason, the cavitation region diagram in the ultrasonic sink is obtained by superposition of the cavitation region diagram at each moment of the half acoustic cycle.

The larger the proportion of the cavitation area, the higher the ultrasonic degradation rate in the plane under certain conditions. Therefore, the pixel method is used to quantitatively compare the areal size of the cavitation area. It is widely known that the image consists of a finite number of pixel points and that the area of the image is proportional to the number of pixel points.[29] Therefore, the size of the cavitation area under different conditions can be quantitatively compared as long as the number of pixel points representing the color of the cavitation region is calculated at a certain resolution.

First, the cavitation area image was imported, and the cavitation area image was binarized using the Binarize function in Mathematica 11.2. After the image is processed, the black areas represent the regions where cavitation occurs, and white represents the regions where no cavitation occurs. The ImageLevels function of the software was employed to count the numbers of pixel points in the image in both black and white colors. Finally, the ratio of the number of black pixels to the sum of the number of black and white pixels was calculated. This ratio represents the percentage of cavitation areas.

3. Results and discussion

3.1. Acoustic field distribution

In the absence of the metal plate, the acoustic field in the water sink undergoes periodic changes over time. This phenomenon is due to the total reflection that occurs when an ultrasonic wave propagates from the base of the ultrasonic tank to the water–air interface. Interference between the reflected acoustic pressure and the incident acoustic pressure forms a standing wave acoustic field, as shown in Figs. 2(a1)

and 2(b1). After the metal plate is added, the acoustic field distributions in the *yz* and *xy* directions are as shown in Figs. 2(a2) and 2(b2). It can be seen that the addition of the metal plate weakens standing waves to a certain extent and improves the distribution of the acoustic field. This is because the presence of the metal plate converts the original acoustic soft boundary at the water–air interface into an acoustic hard boundary and a soft boundary, and total reflection occurs whether the ultrasonic wave propagates to the acoustic hard boundary or the acoustic soft boundary. In addition, the node of the acoustic pressure is formed at the interface when the ultrasound wave reaches the acoustic soft boundary, while the antinode of the acoustic pressure is formed when the ultrasound wave reaches the acoustic hard boundary. Based on the above analysis, when the incident acoustic wave is reflected at the mixed boundary, the reflected sound wave is no longer a plane wave opposite to the incident acoustic wave. As a result, standing waves in the acoustic field are weakened.

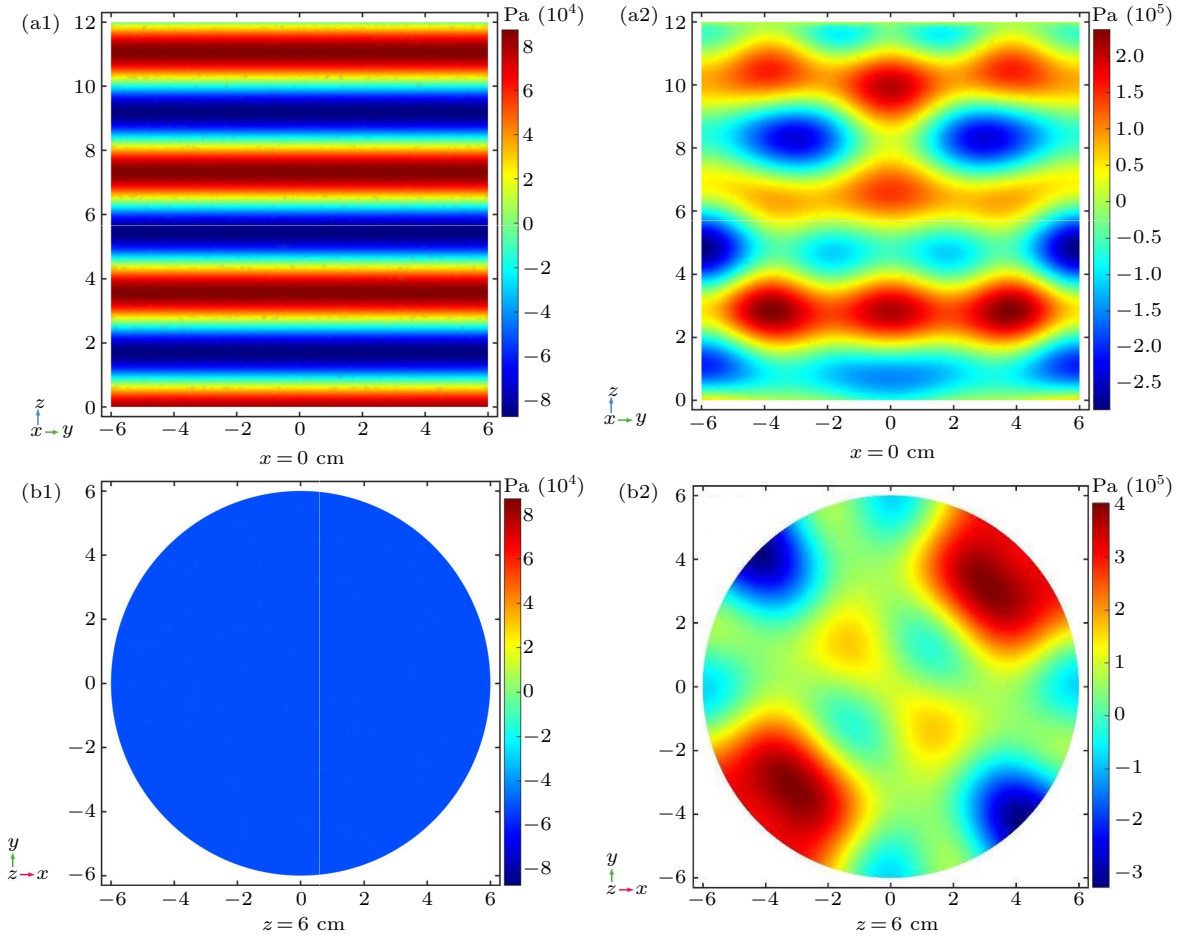


Fig. 2. Acoustic field distribution: (a1) *yz*, $x = 0$ cm, no metal plate; (a2) *yz*, $x = 0$ cm, metal plate; (b1) *xy*, $z = 6$ cm, no metal plate; (b2) *xy*, $z = 6$ cm, metal plate.

3.2. Acoustic pressure at the peak and trough

The analysis in the previous section showed that the acoustic field in the water sink still presents a periodic distribution after the metal plate is added. Therefore, this section examines two points, namely, the antinode and the node of the standing wave field. The changes in acoustic pressure at these two points over time are shown in Figs. 3(a) and 3(b), where the original structure and new structure represent the acoustic pressure without and with the metal plate, respectively. As is evident from the figure, the acoustic pressure at the antinode and node is zero during the period from 0 to 80 μs. This is due to the time required for the ultrasonic wave to reach these points from the bottom of the water sink. In addition, the amplitude of the acoustic pressure tends to be stable after 175 μs, which is due to the time required for the formation of standing waves.

In the *xy* direction of the acoustic field, the antinode and node are selected. They are located at $(z = 12 - \lambda/4)$ cm and $(z = 12 - \lambda/2)$ cm, where λ represents the wavelength of the acoustic wave. This is because the water–air interface is an acoustic soft boundary, and an acoustic pressure wave node is formed at the interface after acoustic reflection. It can be seen in Figs. 3(a) and 3(b) that the acoustic pressure amplitude exceeds the cavitation threshold (1 atm) at both the antinode and node in the presence of the metal plate, while it only exceeds the cavitation threshold at the antinode in the absence of the metal plate. This indicates that the placement of a metal plate at the water–air interface can enlarge the area

of acoustic cavitation in ultrasonic water tanks, which is conducive to the improvement of the acoustic degradation rate. The reason for this is that the acoustic cavitation effect produces hydroxyl radicals.[15] An increase in the cavitation area can increase the concentration of hydroxyl radicals and further improve the ultrasonic degradation rate.[30] In addition, it is found that the acoustic pressure at the antinode without the metal plate is greater than that with the metal plate. This is because, before and after the metal cover plate is added, the incident acoustic pressure remains unchanged, which means that the total sound energy remains constant. After the metal plate is added, the increase in acoustic pressure at the original node leads to a decrease in acoustic pressure at the original antinode. Hatanaka *et al.*[31,32] indicated that multibubble sonoluminescence first increases and then decreases as the ultrasonic power is increased. The double fan-shaped metal plate presented in this paper can reduce the amplitude of the acoustic pressure at the antinode, thus reducing the acoustic power and avoiding the quenching of acoustic cavitation.

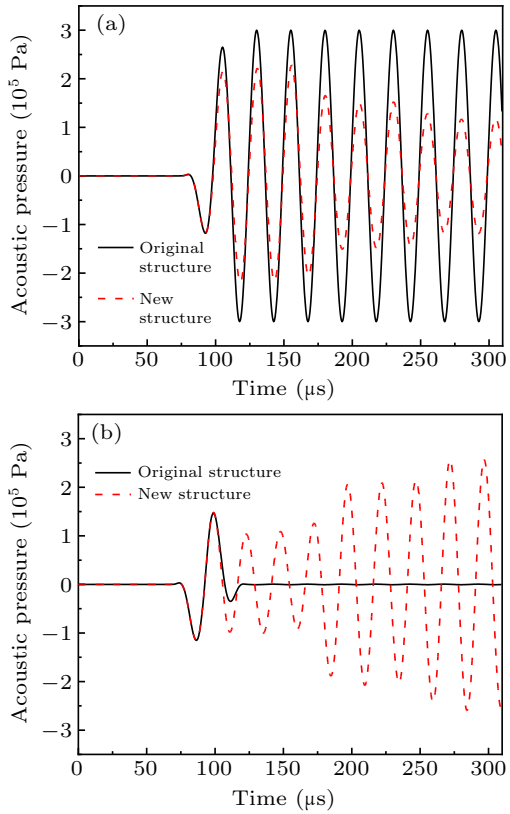


Fig. 3. Acoustic pressure over time at the antinode (a) and the node (b). The original structure represents the acoustic pressure without metal plate, and the new structure represents the acoustic pressure with the metal plate.

3.3. Distribution of cavitation area

To explore the influence of the metal plate on the acoustic cavitation area, three sections were selected in the *yz* direction of the ultrasonic water tank. Based on the cavitation threshold at room temperature and atmospheric pressure, the distribution of the cavitation area across the section was obtained, as illustrated in Fig. 4. The red areas in the figure indicate areas where ultrasonic cavitation occurs. As can be seen in Fig. 4, the cavitation areas on the three sections are distributed in bands when no metal plate is present, while the cavitation areas on the sections are distributed randomly when the metal plate is present. This is because the standing wave acoustic field is formed in the water tank when no metal plate is present, which leads to the banding distribution of the cavitation area on the section. The metal plate could eliminate the standing wave to a certain extent, which leads to the random distribution of the cavitation area on the section.

In addition, it is found that the cavitation areas in the presence of the metal plate are larger than those in the absence of the metal plate. This suggests that the use of the metal plate could enlarge the cavitation area in an ultrasonic water tank and thus improve the ultrasonic degradation rate of organic solutions. This is because the weakening of the standing wave increases the acoustic pressure at the original standing wave node (Fig. 3(b)), thus causing the cavitation effect to occur in regions where it did not occur previously and expanding the regions where the cavitation effect occurs within the ultrasonic tank.

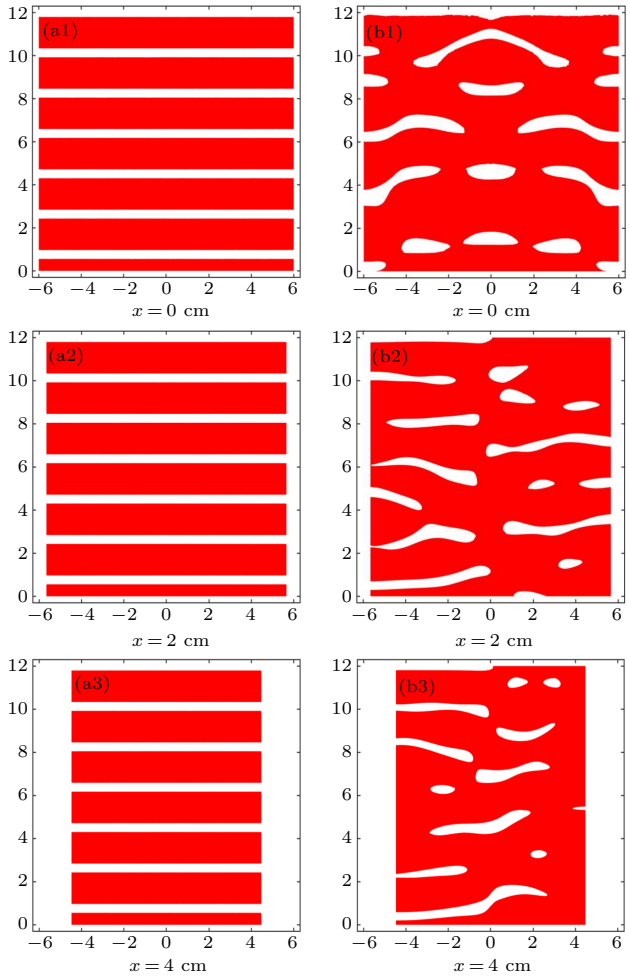


Fig. 4. Cavitation effect areas for different cross sections in the *yz* direction without (a1)–(a3) and with (b1)–(b3) the metal plate. (a1) The area at $x = 0$ cm without the metal plate; (a2) the area at $x = 2$ cm without the metal plate; (a3) the area at $x = 4$ cm without the metal plate; (b1) the area at $x = 0$ cm with the metal plate; (b2) the area at $x = 2$ cm with the metal plate; (b3) the area at $x = 4$ cm with the metal plate.

3.4. Percentage of cavitation area

To quantitatively compare the influence of the metal plate on the cavitation area, the areas of the three sections of the ultrasonic water tank were obtained using the pixel method. When the acoustic pressure amplitude is set to 1.5×10^5 Pa and the liquid level height is 12 cm, the percentages of the cavitation areas of the three sections in the yz direction ($x = 0$ cm, $x = 2$ cm and $x = 4$ cm) under different conditions are as shown in Fig. 5(a). In this figure, the original structure and the new structure represent the cavitation area ratio without and with the metal plate, respectively. The percentage of the cavitation area is defined as the ratio of the area where ultrasonic cavitation occurs to the total area of the section. As can be seen from Fig. 5(a), the percentages of the cavitation areas on the three sections in the presence of the metal plate are greater than those in the absence of the metal plate. This suggests that applying the metal plate at the water–air interface of the ultrasonic cleaning tank can enlarge the area of acoustic cavitation in a certain area, thus further improving the ultrasonic degradation rate of organic solutions in the tank. To verify the accuracy of the calculated results, corresponding ultrasonic degradation experiments were designed, and the experimental results are shown in Figs. 5(b) and 5(c). It can be seen from the figure that adding a metal plate to the ultrasonic tank can improve the degradation rate of the Rhodamine B solution, which confirms the rationality of using the proportion of the cavitation area to evaluate the acoustic degradation rate.

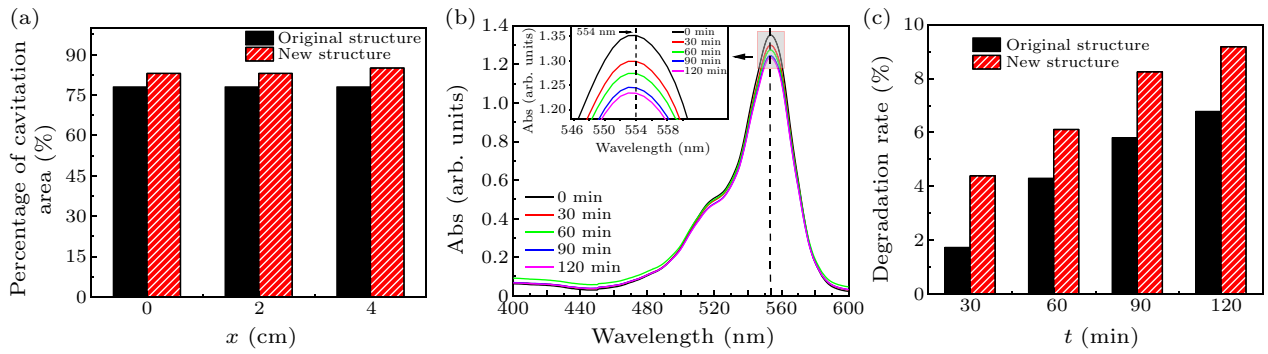


Fig. 5. The effects of the two different structures: (a) percentage of cavitation area on the sections, (b) absorbance of solution over time in a tank with the metal plate, (c) degradation rate of solution under the two different structures.

3.5. Effect of acoustic pressure amplitude on cavitation area proportion

To explore the influence of the acoustic pressure amplitude of the ultrasonic wave emitted from the bottom of the ultrasonic water tank on the percentage of cavitation area on the section, at a liquid level height of 12 cm, the percentages of the cavitation areas on three sections in the yz direction are analyzed under different conditions, as shown in Figs. 6(a)–6(c). It can be seen from Figs. 6(a)–6(c) that the percentages of the cavitation areas on the three sections in the yz direction, in the absence of the metal plate, are equal and increase as the acoustic pressure amplitude grows. There are two reasons for this: one is that the cavitation area in the yz direction in the tank is distributed in bands in the absence of the metal plate, while the other is that the acoustic pressure amplitude of the standing wave acoustic field formed without the metal plate is proportional to the incident acoustic pressure amplitude. The cavitation threshold is a constant value under certain conditions. Therefore, the percentage of the cavitation area on the section in the yz direction increases as the acoustic pressure amplitude grows. In addition, the increasing value of the cavitation area percentage caused by the metal plate first increases and then decreases as the acoustic pressure amplitude grows, and this increasing value is largest when the acoustic pressure amplitude is 2×10^5 Pa. This indicates that under certain conditions, a reasonable acoustic pressure amplitude should be set when the metal plate is used to improve and thus maximize the acoustic degradation rate of the solution in the ultrasonic water tank.

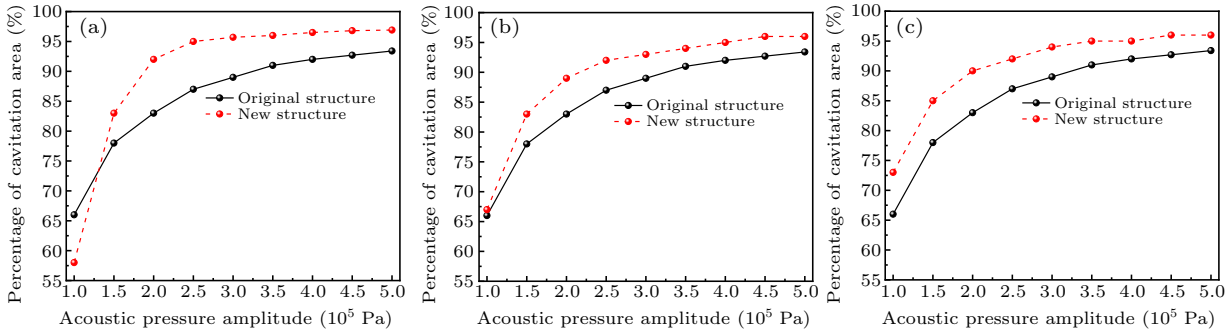


Fig. 6. The effect of the acoustic pressure amplitude on the percentage of cavitation area on the section: (a) $x = 0$ cm, (b) $x = 2$ cm and (c) $x = 4$ cm.

3.6. Effect of liquid height on cavitation area proportion

Thangavadivel *et al.*[33] noted in the literature that the height of the liquid level in the ultrasonic cleaning tank has a significant impact on the ultrasonic degradation rate of organic solutions. When the acoustic frequency is constant, there is an optimal value within a certain range of liquid levels at which the SE value of the organic solution is at a maximum.[34] Therefore, we analyzed the cavitation percentage on three sections in the *yz* direction ($x = 0$ cm, $x = 2$ cm and $x = 4$ cm) with liquid level height in both scenarios. It can be seen in Figs. 7(a)–7(c) that the cavitation area percentage on three sections with the metal plate is greater than that on the section without the metal plate at different liquid level heights. This again demonstrates the advantage of using the metal plate to improve the ultrasonic degradation rate of the solution. It was also found that the percentage of the cavitation area on the three sections in the absence of the metal plate varies sinusoidally with the height of the liquid level, which is basically consistent with the results in the literature.[35] This is because the number of peaks and troughs in the standing wave acoustic field is determined by the liquid level height in the absence of the metal plate, and the ratio of the number of peaks and troughs affects the region where ultrasonic cavitation occurs across the entire section. In addition, it can also be seen that the percentage of the cavitation area in the three sections is basically unaffected by the liquid level change in the presence of the metal plate. The larger the percentage of the cavitation area on the section, the higher the degradation rate of organic solutions under certain conditions. Therefore, it can be concluded that using the metal plate can not only improve the acoustic degradation rate of organic solutions, but also eliminate the influence of the height of the liquid level in the ultrasonic tank on the acoustic degradation rate of the organic solution, thereby further improving the efficiency of ultrasonic degradation.

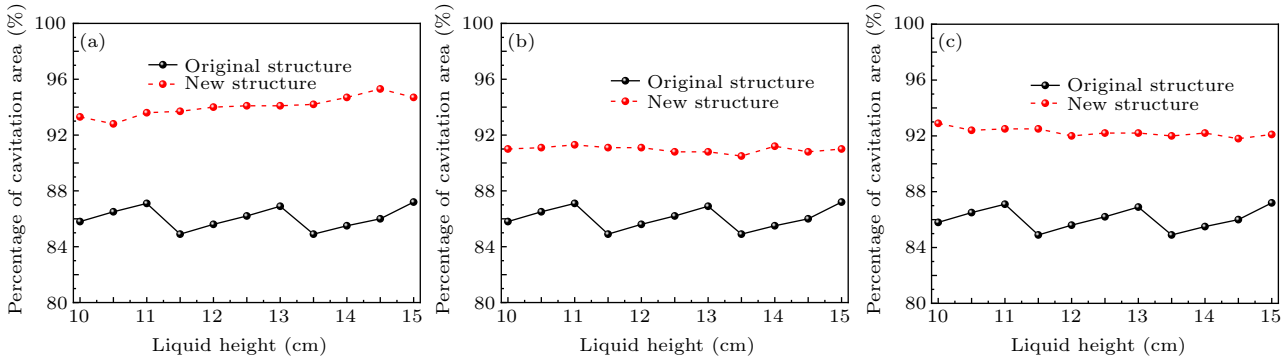


Fig. 7. The effect of liquid height on the percentage of cavitation area on the section: (a) $x = 0$ cm, (b) $x = 2$ cm and (c) $x = 4$ cm.

3.7. Effect of acoustic frequency on cavitation area proportion

To explore the effect of acoustic frequency on the acoustic cavitation area in the ultrasonic flume, three cross sections were selected in the *yz* direction of the flume ($x = 0$ cm, $x = 2$ cm and $x = 4$ cm). The percentages of the cavitation areas on the three sections in the *yz* direction at different frequencies are shown in Figs. 8(a)–8(c) for an acoustic pressure amplitude of 2×10^5 Pa and a liquid level height of 12 cm. It can be seen from the figure that at all frequencies except 25 kHz, the proportions of the acoustic cavitation areas on the three cross sections with the metal cover plate are greater than those without the metal cover plate. In addition, it is found that the metal cover shows the most obvious effect on the proportion of the acoustic cavitation area in the water tank when the frequency of the acoustic wave is in the range of 35 kHz to 45 kHz. Therefore, when the metal cover plate is used, it is necessary to select the appropriate acoustic frequency to improve the proportion of the acoustic cavitation area.

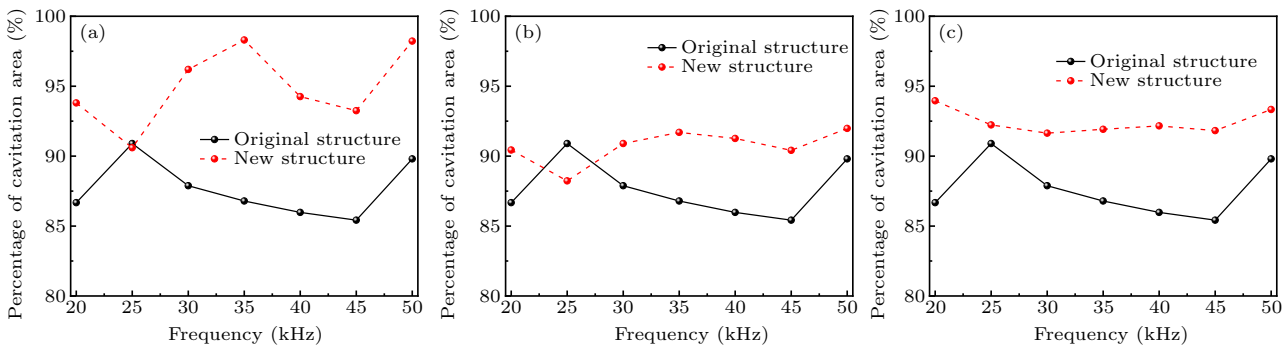


Fig. 8. The effect of frequency on the percentage of cavitation area on the section: (a) x =0 cm, (b) x =2 cm and (c) x =4 cm.

4. Conclusions and perspectives

In order to further enhance the degradation rate of the organic solution, a metal plate with a certain shape was proposed to be placed at the water–air interface of the ultrasonic water tank. The simulation results indicated that the addition of the metal plate can eliminate the standing wave acoustic field to a certain extent and improve the amplitude of the acoustic pressure at the troughs of the standing wave acoustic field, thus enlarging the area of ultrasonic cavitation in the ultrasonic cleaning tank. To further quantitatively analyze the influence of the metal plate on the ultrasonic cavitation area, the area of ultrasonic cavitation in the water tank was obtained through the pixel method based on the cavitation threshold under certain conditions. The calculation results demonstrate that the presence of the metal plate can increase the area of ultrasonic cavitation in the water tank. The corresponding experimental ultrasonic degradation results confirmed the feasibility of using the proportion of the cavitation area to evaluate the degradation rate. In addition, the effects of acoustic pressure amplitude, liquid level height, and acoustic frequency on the area of ultrasonic cavitation were also explored. Based on the calculation results, the following conclusions are drawn: first, a reasonable acoustic pressure amplitude should be set when the metal plate is used to improve the acoustic degradation rate of the solution in the ultrasonic water tank, in order to maximize the increase in the acoustic degradation rate; second, placing the metal plate can not only improve the acoustic degradation rate of organic solutions but also eliminate the influence of the height of the liquid level in the ultrasonic tank on the acoustic degradation rate of the organic solution. Therefore, the method for improving the ultrasonic degradation rate of organic solutions proposed in this paper is simple, energy-saving, and eco-friendly and provides a powerful theoretical basis for the large-scale market application of the ultrasonic degradation method.

Acknowledgments

Project supported by the Doctoral Fund Program of Longdong University (Grant No. XYBYZK2219), the National Natural Science Foundation of China (Grant No. 12274277), the Science and Technology Project of Gansu Province of China (Grant No. 21JR11RM046), and Young Doctor Fund of Gansu Education Department (Grant No. 2022QB-171).

References

[1] Shen Z H 2005 *China Biogas* **23** 161 (in Chinese)
[2] Xue S 2023 *Sustainable Mining and Metallurgy* **39** 63
[3] Kiso Y, Sugiura Y, Kitao T and Nishimura K 2001 *J. Membr. Sci.* **192** 1
[4] Wang Y, Rao G Y and Hu J Y 2011 *Water Sci. Technol.: Water Supply* **11** 711
[5] Alexander J T, Hai F I and Al-Aboud T M 2012 *J. Environ. Manage* **111** 195
[6] Sala M and Gutiérrez-Bouzán M C 2012 *Int. J. Photoenergy* **2012** 1
[7] Zhang M, Shi Q, Song X, Wang H and Bian Z 2019 *Environ. Sci. Pollut. Res.* **26** 10457
[8] Ahmady-Asbchin S, Andres Y, Gerente C and Le Cloirec P 2009 *Environ. Technol* **30** 755
[9] Al-Gheethi A A, Lalung J, Noman E A, Bala J and Norli I 2015 *Clean Technol. Environ. Policy* **17** 2101
[10] Von Sonntag C 2008 *Water Sci. Technol.* **58** 1015
[11] Vilar V J, Malato S and Dionysiou D D 2015 *Environ. Sci. Pollut. Res.* **22** 759
[12] Kitano M and Hara M 2010 *J. Mater. Chem.* **20** 627
[13] Xiong Z K, Zhang H, Zhang W C, Lai B and Yao G 2019 *Chem. Eng. J.* **359** 13
[14] Radi M A, Nasirizadeh N, Rohani-Moghadam M and Dehghani M 2015 *Ultrason. Sonochem.* **27** 609
[15] Ikehata K and Gamal El-Din M 2005 *OZSE* **27** 173
[16] Amritha A S and Manu B 2016 *Water. Sci. Technol* **74** 1919
[17] Wang J, Wang Z J, Vieira C L Z, Wolfson J M, Pingtian G and Huang S D 2019 *Ultrason. Sonochem.* **55** 273
[18] Tyagi V K, Lo S L, Appels L and Dewil R 2014 *Crit. Rev. Environ. Sci. Technol.* **44** 1220
[19] Wu W H, Zhai W, Hu H B and Wei B B 2017 *Acta Phys. Sin.* **66** 194303 (in Chinese)
[20] Ren J L, Zhang M D, Niu Y and Lin C P 2003 *Piezoelect. Acoustoopt.* **25** 347
[21] Wei Z S and Weavers L K 2016 *Ultrason. Sonochem.* **31** 490
[22] Zhang Z B, Gao T T, Liu X Y, Li D W, Zhao J W, Lei Y Q and Wang Y K 2018 *Ultrason. Sonochem.* **42** 787
[23] Rashwan S S, Dincer I and Mohany A 2020 *Ultrason. Sonochem.* **68** 105174
[24] Liu J H, Shen, Z Z, and Lin S Y 2021 *Chin. Phys. B* **30** 104302
[25] Zhai W, Liu H M, Hong Z Y, Xie W J and Wei B 2017 *Ultrason. Sonochem.* **34** 130
[26] Tiong T J, Price G J and Kanagasingam S 2014 *Ultrason. Sonochem.* **21** 1858
[27] Marmottant P, Versluis M, de Jong N, Hilgenfeldt S and Lohse D 2005 *Exp. Fluids* **41** 147
[28] Guédra M, Cornu C and Inserra C 2017 *Ultrason. Sonochem.* **38** 168
[29] Wen N, Snyder K, Scheib S, Qin Y, Li H and Chetty I J 2016 *Med. Phys.* **43** 3448
[30] Nie G, Hu K, Ren W, Zhou P, Duan X, Xiao L and Wang S 2021 *Water. Res.* **198** 117
[31] Hatanaka S I, Yasui K, Kozuka T, Tuziuti T and Mitome H 2002 *Ultrason. Sonochem.* **40** 655
[32] Hatanaka S I, Yasui K, Kozuka T, Tuziuti T and Mitome H 2001 *Jpn. J. Appl. Phys.* **40** 3856
[33] Thangavadivel K, Okitsu K, Owens G, Lesniewski P J and Nishimura R 2013 *J. Environ. Chem. Eng.* **1** 275
[34] Asakura Y, Nishida T, Matsuoka T and Koda S 2008 *Ultrason. Sonochem.* **15** 244
[35] Son Y, Lim M, Ashokkumar M and Khim J 2011 *J. Phys. Chem. C* **115** 4096